High-spin states in ^{114}Sn

H. Harada*
Department of Physics, Tokyo Institute of Technology, Tokyo 152, Japan

M. Sugawara
Chiba Institute of Technology, Narashino 275, Japan

H. Kusakari, H. Shinohara, and Y. Ono
Faculty of Education, Chiba University, Chiba 260, Japan

K. Furuno and T. Hosoda
Institute of Physics, University of Tsukuba, Tsukuba 305, Japan

M. Adachi
Department of Applied Physics, Tokyo Institute of Technology, Tokyo 152, Japan

S. Matsuki
Chemical Research Institute, Kyoto University, Kyoto 606, Japan

N. Kawamura
Department of Physics, Tohoku University, Sendai 980, Japan
(Received 18 July 1988)

The single-closed-shell nucleus ^{114}Sn was studied using the ^{100}Mo(^{18}O,4n) reaction. High-spin deformed states in ^{114}Sn were observed up to the (22^+) state, and the backbending phenomenon was found. Constancy in the moment of inertia for the high-spin states was observed. The calculation based on the spin-projection Hartree-Bogoliubov model reproduces well the experimental data. The backbending phenomenon in ^{114}Sn is explained as due to the band crossing between the intruder g band and the intruder aligned $(\nu h_{11/2})^2$ band.

I. INTRODUCTION

Deformed states have been observed in closed- or nearly-closed-shell nuclei.[1-6] These states form a rotational-like band and can be distinguished from spherical states of quasiparticle excitation. We call these bands in the spherical region by the name of "intruder bands;" the low-lying (low-spin) intruder band is called the intruder g band. In the Sn isotopes it has been interpreted as a consequence of the two-particle two-hole excitation across the proton closed shell[1] in terms of the spherical shell model. Recently, the upbending phenomenon for the intruder band in ^{112}Sn has been observed.[6] This phenomenon was considered to be caused by the band crossing between the intruder g band and the intruder aligned band:[6,7] The second intruder band is formed by the rotation alignment in the two-quasineutron $(\nu h_{11/2})^2$ state from the intruder g band.[7] The intruder bands in ^{110,112}Sn and the upbending phenomenon in ^{112}Sn have been well reproduced by the spin-projection Hartree-Bogoliubov model including the $(\nu h_{11/2})^2$ quasiparticle excitation.[7] One of the most striking features of the intruder aligned $(\nu h_{11/2})^2$ bands in ^{110,112}Sn is that the values of their moment of inertia remain almost constant at high rotational frequencies 0.4 MeV $< \hbar\omega <$ 0.6 MeV.[5,6] Similar phenomenon has been observed in some deformed nuclei.[8-11] Much interest has been focused on them. However, microscopic understanding of the constancy in the moment of inertia has not been satisfactory. Extended investigation for the systematics would thus provide a sequence of important tests for theoretical approaches to the observed rotational-like bands in the spherical region.

We have investigated high-spin states in ^{114}Sn to obtain more systematic data on the feature of band crossing and also to test the constancy in the moment of inertia for the intruder band at high rotational frequencies in the heavier Sn isotopes. We have done the nuclear spectroscopic study using the ^{100}Mo(^{18}O,4n)^{114}Sn reaction and made a calculation based on the spin-projection Hartree-Bogoliubov model for ^{114}Sn.

In the previous work[3,4] on ^{114}Sn, the intruder band has been investigated up to the 12^+ state at 5548 keV; excited states have been observed up to the 6046 keV level.

II. METHODS OF EXPERIMENT AND ANALYSIS

High-spin states in ^{114}Sn were populated using the ^{100}Mo(^{18}O,4n) reaction at a beam energy of 65 MeV. The

^{18}O beam was provided by the sector focusing (SF) cyclotron at the Institute for Nuclear Study (INS) of the University of Tokyo. The Mo target isotopically enriched to 96% in ^{100}Mo was a 2 mg/cm^2 thick foil with a lead backing. Gamma-gamma coincidences were measured with a γ-ray spectrometer array consisting of six bismuth-germanate (BGO) anti-Compton spectrometers (BGOACS's) in which each Ge detector was surrounded by the BGO anti-Compton shield.[12] The BGOACS's were arranged at 0°, 45°, 90°, 145°, −105°, and −155° to the beam direction. The Ge detectors were set about 17 cm away from the target. The lead collimator of 4 cm thickness was set between each detector and the target. Sixty million events were recorded under the condition that pulses from two or more BGOACS's were in coincidence.

The γ rays of ^{114}Sn have been located in the level scheme using the observed coincidence relationship and the intensity argument for γ rays. We have evaluated the following ratio for each possible multipolarity of the gated transition (γ_1) and the gating transition (γ_2):

$$R^{\text{calc}} = A/B \ , \tag{1}$$

$$A = \sum W(\theta_1,\theta_2)\epsilon_{\gamma 1}(\theta_1)\epsilon_{\gamma 2}(\theta_2) \quad \begin{bmatrix}\theta_1 = 90°, -105° \\ \theta_2 = 0°, 45°, 145°, -155°\end{bmatrix} ,$$

$$B = \sum W(\theta_1,\theta_2)\epsilon_{\gamma 1}(\theta_1)\epsilon_{\gamma_2}(\theta_2) \quad \begin{bmatrix}\theta_1,\theta_2 = 0°, 45°, 145°, -155° \\ \theta_1 \neq \theta_2\end{bmatrix} ,$$

where $W(\theta_1,\theta_2)$ is the theoretical $\gamma\gamma$ angular correlation function,[13] and $\epsilon_\gamma(\theta_i)$ is the detection efficiency for each detector which was calibrated by the ^{152}Eu source set at the target position. The ratios calculated by Eq. (1) are $1.65 \sim 1.81$ for γ_1 with a stretched dipole character and $0.69 \sim 0.77$ for γ_1 with a stretched quadrupole character;

TABLE I. Excitation energies E_{ex}, transition energies E_γ, assignments of $I_i \rightarrow I_f$, relative intensities I_γ and angular correlation ratios R^{expt} in ^{114}Sn.

E_{ex} (keV)	E_γ (keV)	$I_i \rightarrow I_f$		I_γ	R^{expt}
1299.9	1299.9(3)	2^+	0^+	1000	0.86(3)
2187.9	888.0(3)	4_1^+	2^+	692(22)	0.91(1)
2275.4	975.5(3)	3^-	2^+	75(12)	1.20(11)
2614.0	1314.1(3)	4_2^+	2^+	196(7)	0.94(4)
	375.1(4)	4_2^+	(2^+)	12(2)	0.94(19)
2765.1	1465.1(3)	4_3^+	2^+	12(3)	
2815.8	628.0(3)	5^-	4_1^+	508(22)	1.33(4)
	540.2(3)	5^-	3^-	96(8)	
3088.1	272.3(3)	7^-	5^-	548(17)	0.78(2)
3188.5	1001.2(3)	6^+	4_1^+	43(4)	0.89(11)
	574.3(3)	6^+	4_2^+	164(4)	0.87(4)
	423.0(5)	6^+	4_3^+	15(2)	0.53(18)
3191.1	103.0(3)	8^-	7^-	144(4)	1.26(6)
3511.4	320.3(3)	9^-	8^-	282(11)	0.93(2)
3870.8	682.3(3)	8^+	6^+	176(4)	0.77(2)
4140.4	629.0(5)	$10_1^{(+)}$	9^-	200(22)	1.38(4)
4672.5	801.7(3)	10_2^+	8^+	138(5)	0.82(4)
4963.9	1452.5(3)		9^-	48(3)	
5182.7	1042.3(3)	$12_1^{(+)}$	$10_1^{(+)}$	188(4)	0.75(2)
5548.0	875.5(3)	12_2^+	10_2^+	76(4)	0.88(4)
5922.1	739.4(3)	$14_1^{(+)}$	$12_1^{(+)}$	40(3)	0.62(8)
6046.3	863.6(3)	$14_2^{(+)}$	$12_1^{(+)}$	106(4)	0.70(4)
	124.4(5)	$14_2^{(+)}$	$14_1^{(+)}$	< 10	
6267.0	344.9(3)		$14_3^{(+)}$	15(1)	1.08(17)
6341.2	793.2(3)	14_3^+	12_2^+	44(4)	0.68(5)
6551.6	505.3(3)		$14_2^{(+)}$	64(3)	0.90(6)
	284.5(3)			7(1)	1.10(20)
6925.5	878.9(8)		$14_2^{(+)}$	< 10	
	374.1(3)			22(2)	1.05(15)
7205.1	1159.4(3)	16^+	$14_2^{(+)}$	63(4)	0.89(7)
	863.4(3)	16^+	14_3^+	40(4)	0.68(6)
8142.6	937.5(4)	18^+	16^+	27(3)	0.91(12)
9195.8	1053.2(7)	(20^+)	18^+	13(1)	
10 359.8	1164.0(10)	(22^+)	(20^+)	10(1)	

the ranges in the calculated ratios are due to the variations caused by the condition that the observed transition energies of γ_1 and γ_2 are from 200 to 1600 keV, and they also include the effect of the multipolarity of gating transition γ_2. If the attenuation of spin alignment[14] is taken into account (for instance the reasonable population of alignment $\sigma = 1.0 \sim 2.4$ is introduced here), the above ratios become $1.30 \sim 1.75$ and $0.70 \sim 1.0$, respectively. The experimental function of $\gamma\gamma$ angular correlation, $Y(\theta_1, \theta_2)$, corresponds to

$$W(\theta_1, \theta_2)\epsilon_{\gamma 1}(\theta_1)\epsilon_{\gamma 2}(\theta_2)$$

in Eq. (1) and has been measured in the present experiment. The experimental ratio R^{expt} has been obtained by substituting $Y(\theta_1, \theta_2)$ for

$$W(\theta_1, \theta_2)\epsilon_{\gamma 1}(\theta_1)\epsilon_{\gamma 2}(\theta_2)$$

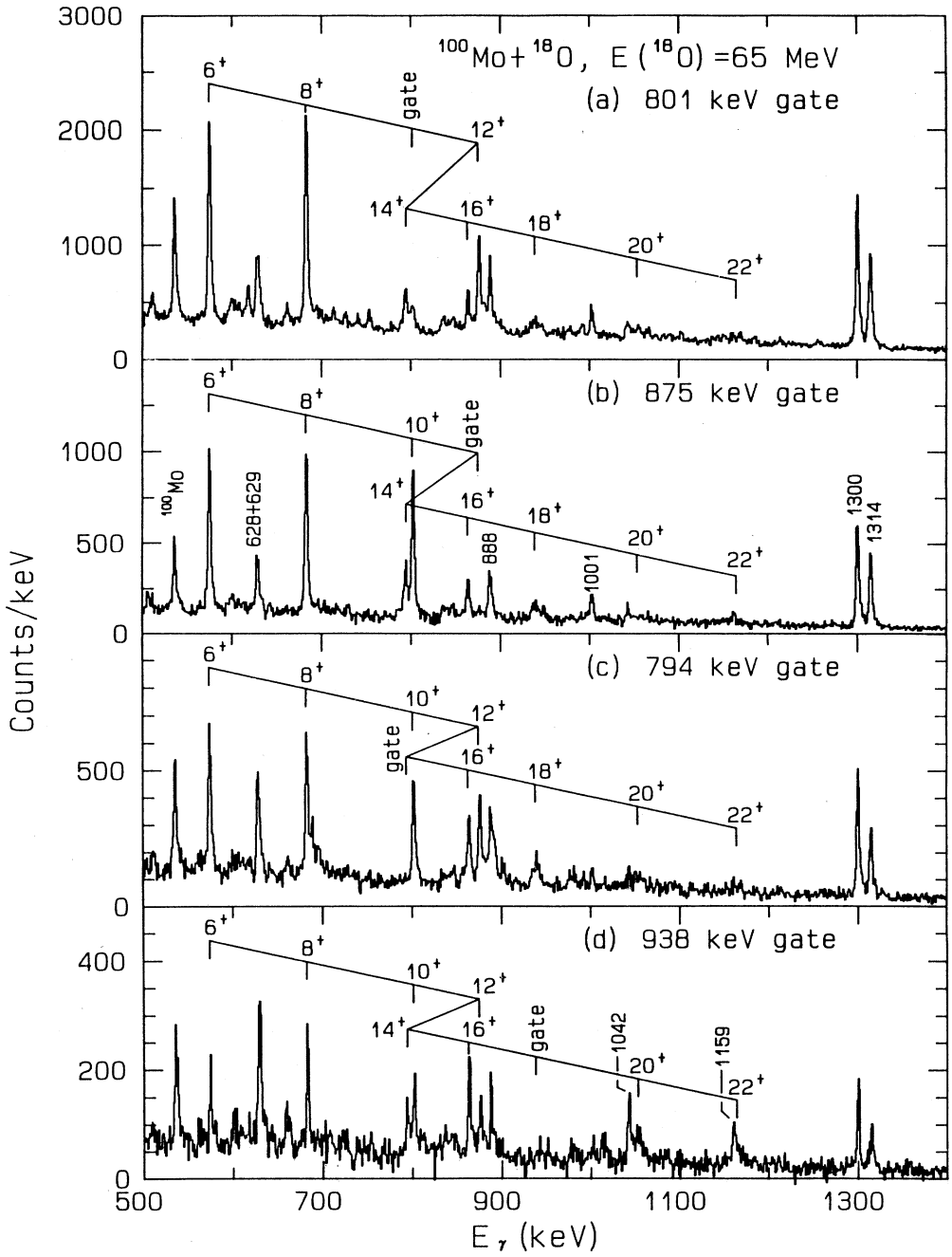

FIG. 1. The $\gamma\gamma$ coincidence spectra for the following gate transitions: (a) 801 keV $10^+ \rightarrow 8^+$, (b) 875 keV $12^+ \rightarrow 10^+$, (c) 794 keV, and (d) 938 keV. Note that the peaks for the $(20^+) \rightarrow 18^+$ and $(22^+) \rightarrow (20^+)$ transitions are broadened by the Doppler effect.

in Eq. (1). The calculated ratio ($0.7 \sim 1.0$) for the stretched quadrupole is almost consistent with the experimental ratios for the previously known stretched-$E2$ transitions in ^{114}Sn (see Table I). Transition multipolarities have been determined by comparing the experimental ratios (R^{expt}) with the calculated ratios (R^{calc}). Present spin assignments based on the $\gamma\gamma$ angular correlation data are shown in Table I.

III. EXPERIMENTAL RESULTS

Figure 1(a) and (b) shows the spectra in coincidence with the 801 keV $10^+ \rightarrow 8^+$ and 875 keV $12^+ \rightarrow 10^+$ transitions in the intruder band of ^{114}Sn. The spectra in coincidence with the 794 and 938 keV γ rays are also shown in Fig. 1(c) and (d). A new sequence of the 794, 863, 938, 1053, and 1164 keV γ rays was observed just above the intruder 12^+ state at 5548 keV; the new levels are proposed at 6341, 7205, 8143, 9196, and 10 360 keV. The angular correlation data are consistent with the 794, 863, and 938 keV γ rays having a stretched-$E2$ character. Therefore, the 6341, 7205, and 8143 keV levels are identified as the 14^+, 16^+, and 18^+ states, respectively; the assignment of the positive parity for these states is based on the rotational-like feature of level energies and their systematics[6] in the Sn isotopes. The multipolarity information for the 1053 and 1164 keV transitions was not obtained because of their Doppler broadenings and weak γ-ray intensities. The *possible* spin-parity assignments of 20^+ and 22^+ to the 9196 and 10 360 keV levels, respectively, are proposed on the basis of the fact that these levels follow the $I(I+1)$ rule assuming the above spin values.

The negative-parity spherical states have been reported up to the 3511 keV 9^- state.[4] They are confirmed by the present experimental data. The 4139 keV level was as-

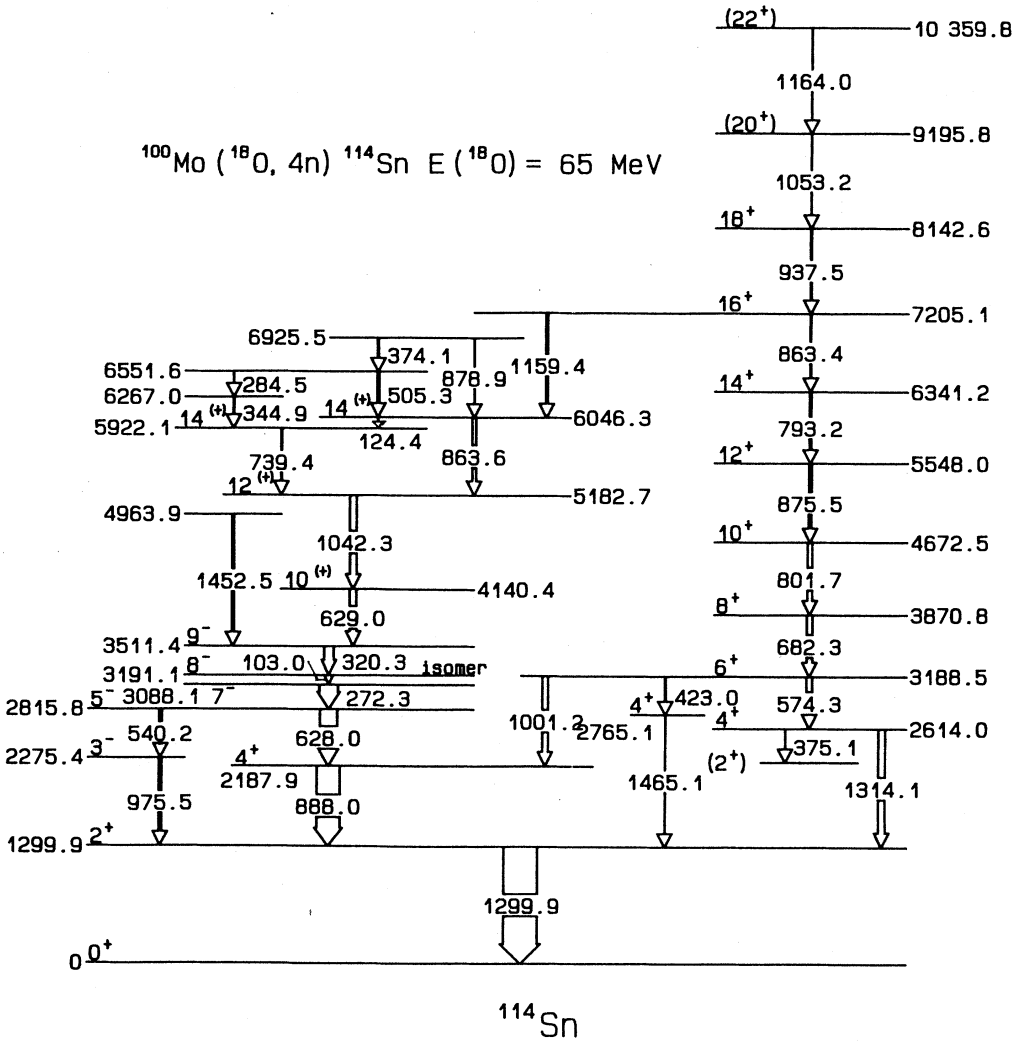

FIG. 2. Level scheme of ^{114}Sn which has been obtained from the present experiment. Intensities of γ rays following the ^{100}Mo(^{18}O,$4n$) reaction at 65 MeV are also shown by the width of arrow. Previous spin-parity assignments for lower-spin states are explained in the text.

signed tentatively as a 10^+ state in the previous work.[4] The assignment of spin 10 to this level is confirmed on the basis of the experimental result from the angular correlation data (see Table I). The previous work[4] proposed also the 5183, 5922, and 6046 keV levels. In the present experiment, the 124 keV transition feeding the 5922 keV level has been observed; the 6046 keV level is confirmed. The assignments of $12^{(+)}$, $14^{(+)}$, $14^{(+)}$ to the 5183, 5922, and 6046 keV levels are based on the fact that the angular correlation ratios (R^{expt}) for the 1042, 739, and 864 keV γ rays are consistent with of the stretched-quadrupole type. The 6046 keV level is fed partly from the 7205 keV 16^+ level through the 1159 keV transition [see Figs. 2 and 3(b)]. The $14^{(+)}$ assignment to the 6046 keV level is also consistent with the fact that the 1159 keV transition is of the stretched-quadrupole type. The three levels at 6267, 6552, and 6926 keV are proposed on the basis of the 345, 285, 505, 374, 879 keV transitions [see Figs. 3(a) and (b)].

IV. DISCUSSION

Members of the rotational-like band in ^{114}Sn has been observed up to the (22^+) state in the present experiment. The energy spacings between the high-spin ($I > 14$) members increase monotonously with their spin values. In Fig. 4(a), circles connected by solid lines show the experimental moment of inertia J as a function of the square of rotational frequency $(\hbar\omega)^2$. The abrupt increase of the moment of inertia is seen at the angular frequency $\hbar\omega \sim 0.41$ MeV. For comparison, the experimental data[5,6] in ^{110,112}Sn are also shown in Fig. 4(b). Compared with the intruder band in ^{112}Sn, the backbending frequency $\hbar\omega$ in ^{114}Sn is higher and the backbending is more abrupt. Another interesting feature in ^{114}Sn is the constancy of the moment of inertia for the high-spin ($I \geq 16$) members of the band. This character is also seen in ^{110}Sn and ^{112}Sn. The saturated value of the moment of inertia in ^{114}Sn is very close to the values in ^{110,112}Sn as shown in Fig. 4. The ratio B/A for these high-spin states is about -3×10^{-5}, where the coefficients A and B are given in the expansion of the excitation energy in terms of the angular momentum:

$$E_I = AI(I+1)+B[I(I+1)]^2+C \ .$$

This ratio is as small as those for the rotational bands which are regarded as a very good rotor[8-11] in the rare-earth nuclei.

We have employed the spin-projection Hartree-Bogoliubov model[7,15] to examine the backbending

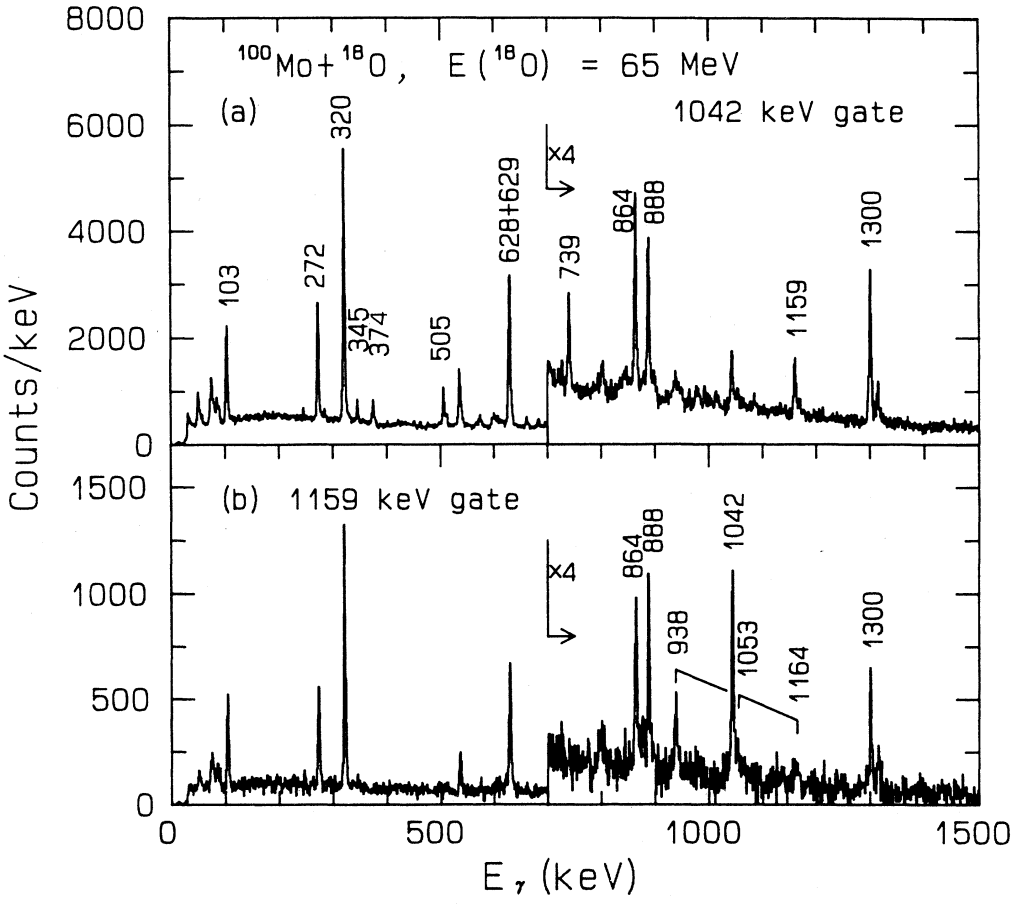

FIG. 3. The $\gamma\gamma$ coincidence spectra for the following gate transitions: (a) 1042 keV and (b) 1159 keV.

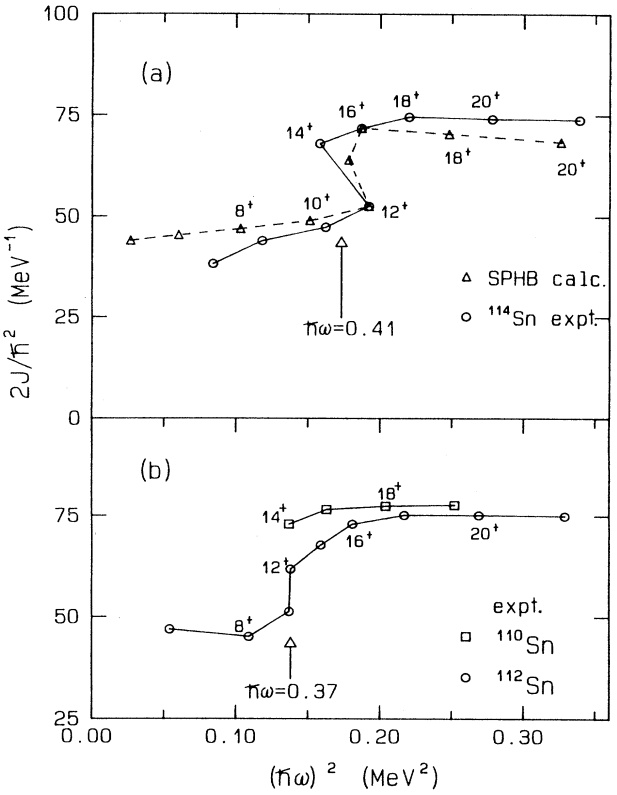

FIG. 4. Plots of the moment of inertia as a function of the square of rotational frequency: (a) for ^{114}Sn and (b) for ^{110,112}Sn (from Ref. 6). Solid lines show the experimental data, and dashed lines the calculations using the spin-projection Hartree-Bogoliubov model.

phenomenon observed in ^{114}Sn. Three major shells for both neutrons and protons are included in the present calculation. The Hamiltonian is the type of single-particle plus pairing plus quadrupole-pairing plus QQ force:

$$\hat{H}=\hat{h}-G\hat{P}^{+}\hat{P}-G_Q\Sigma\hat{P}^{+}_k\hat{P}_k-\tfrac{1}{2}\chi\Sigma\hat{Q}^{+}_k\hat{Q}_k \ . \quad (2)$$

A detailed description of the calculation method can be seen in Ref. 7. The interaction strength used in this calculation was chosen in the same way as in Ref. 7: $G^{(\pi)}=0.172$ MeV, $G^{(\nu)}=0.155$ MeV, $G_Q=0.2G$, and $\chi=3.65\times10^{-3}$ fm^{-4} MeV. The calculated energy surface is similar to that reported in Ref. 7 and has two local minima: the first minimum for the spherical state and the second minimum for the prolate deformation. Triangles connected by dashed lines in Fig. 4(a) show the calculated moment of inertia for the prolate-deformed band. The present calculation reproduces well the feature of backbending, i.e., the band-crossing frequency $\hbar\omega$ and the amount of change of the moment of inertia. This suggests that the backbending phenomenon observed in ^{114}Sn is caused by the band crossing between the intruder g band and the intruder aligned band. According to the present calculation, the two-quasineutron $(vh_{11/2})^2$ component becomes dominant in the intruder aligned band after the band crossing ($I>14$). The present calculated values of transition energies for high-spin ($I\geq18$) intruder states are about 100 keV larger than the experimental values. The inclusion of a variable pairing force as a function of spin and the effect of four-quasiparticle excitations might make this discrepancy small.

The noncollective excited states with spin $I\leq10$ in the even-mass Sn isotopes are systematically interpreted to be fairly pure two-quasiparticle states;[4,16,17] the 4140 keV $10^{(+)}$ state in ^{114}Sn follows the systematic trend of the $(vh_{11/2})^2_{10^+}$ state in the Sn isotopes. Interpretation of the $12^{(+)}$ state at 5182 keV as a two-quasiparticle excitation coupled to the spherical 2^+_1 state was proposed in view of the fact that this excitation energy is about 1 MeV higher than the spherical $10^{(+)}$ state at 4140 keV to which it decays.[4] In analogy to this, either of the $14^{(+)}$ states at 5922 and 6046 keV is expected to have mainly $(vh_{11/2})^2_{10^+}\otimes4^+_1$ configuration. Therefore, these spherical states with $I=12$ or 14 are considered to be four-quasineutron states.

The excitation energies of the four-quasineutron states with $12^{(+)}$ or $14^{(+)}$ are about 300 keV lower in comparison with the 12^+ or 14^+ states of the intruder aligned band. At higher excitation energies than the 7205 keV 16^+ state, the intensities of the intraband transitions in the intruder aligned band become most intensive. This means that the phase transition from the spherical shape to the deformed shape occurs around spin $I=16$ along the yrast line. It is expected in ^{114}Sn that a deformed 16^+ state is close to a spherical 16^+ state and that the 16^+ state at 7205 keV has the mixture of both components. The present experimental data shows that the branching to the deformed 14^+ state and the spherical $14^{(+)}$ state occurs in the decay of the 7205 keV 16^+ state.

V. CONCLUSION

High-spin states in the single-closed-shell nucleus ^{114}Sn have been investigated using the γ-ray spectroscopic technique following the ^{100}Mo(^{18}O,4n) reaction. The deformed states have been observed from 4^+ to (22^+) in the present experiment; they are members of the intruder band. We have found the backbending phenomenon at the rotational frequency $\hbar\omega\sim0.41$ MeV in this band. This phenomenon is proposed as due to the band crossing between the intruder g band and the intruder aligned $(vh_{11/2})^2$ band on the basis of the calculation using the spin-projection Hartree-Bogoliubov model. The present microscopic calculation reproduces well the backbending phenomenon in the intruder band of ^{114}Sn. The constancy in the moment of inertia is seen for the intruder aligned band at higher rotational frequency $\hbar\omega\geq0.44$ MeV. This saturated value of the moment of inertia is almost equal to those in ^{110,112}Sn.

In addition to the above deformed states, noncollective high-spin states were observed up to the $14^{(+)}$ state. We propose that these states are neutron four-quasiparticle states.

ACKNOWLEDGMENTS

The authors wish to thank Dr. Y. Gono for valuable discussion and Dr. S. Iwasaki for his support of the theoretical calculation. They are also grateful to Professor M. Ishihara for convenience in using the BGO anti-Compton spectrometer and to the INS SF-cyclotron crew for the preparation of a ^{18}O beam.

---

*Present address: Frontier Group, Power Reactor and Nuclear Fuel Development Corporation, Tokai-mura, Japan.

[1]K. Heyde, P. Van Isacker, M. Waroquier, J. L. Wood, and R. M. Meyer, Phys. Rep. **102**, 291 (1983).
[2]J. H. Hamilton *et al.*, Rep. Prog. Phys. **48**, 631 (1985).
[3]J. Bron *et al.*, Nucl. Phys. **A318**, 335, (1979).
[4]A. Van Poelgeest, J. Bron, W. H. A. Hesselink, K. Allaart, J. J. A. Zalmstra, M. J. Uitzinger, and H. Verheul, Nucl. Phys. **A346**, 70 (1980).
[5]D. A. Viggars, H. W. Taylor, B. Singh, and J. C. Waddington, Phys. Rev. C **36**, 1006 (1987).
[6]H. Harada, T. Murakami, K. Yoshida, J. Kasagi, T. Inamura, and T. Kubo, Phys. Lett. B **207**, 17 (1988).
[7]S. Iwasaki, Prog. Theor. Phys. **79**, 730 (1988).
[8]R. Chapman *et al.*, Phys. Rev. Lett. **51**, 2265 (1983).
[9]E. M. Beck *et al.*, Nucl. Phys. **A464**, 472 (1987).
[10]J. C. Bacelar *et al.*, Nucl. Phys. **A442**, 509 (1985).
[11]J. Recht *et al.*, Nucl. Phys. **A440**, 366 (1985).
[12]M. Fukuda *et al.*, RIKEN Accel. Prog. Rep. **18**, 152 (1984).
[13]D. Pelte and D. Schwalm, in *Heavy Ion Collisions,* edited by R. Bock (North-Holland, Amsterdam, 1982), Vol. 3, Chap. 1.
[14]T. Yamazaki, Nucl. Data **A3**, 1 (1967).
[15]K. Hara and S. Iwasaki, Nucl. Phys. **A332**, 61 (1979); **A348**, 200 (1980).
[16]G. Bonsignori, M. Savoia, K. Allaart, A. van Egmond, and G. Te Velde, Nucl. Phys. **A432**, 389 (1985).
[17]J. Kasagi, H. Harada, T. Murakami, K. Yoshida, H. Tachibanaki, and T. Inamura, Phys. Lett. B **176**, 307 (1986).